Supporting Information

A Facile Co-Assembly Process to Generate Core-Shell Nanoparticles with Functional Protein Corona

Nisaraporn Suthiwangcharoen, Tao Li, Laying Wu, Heidi B. Reno, Preston A. Thompson, Qian Wang

Email: wang263@mailbox.sc.edu

Table S1. Basic properties of proteins used as building blocks and the complexes formed between proteins and P4VP at pH 7.4. C and A means colloids and aggregates, respectively.

Protein	Mw (kDa)	pI	P4VP
Pepsin (Pep)	35	2.8	C
Porcine stomach mucin (Psm)	103	4.4	C
Ferritin (Fer)	750	4.5	C
Concanavalin A (Con A)	104	4.5	C
Gelatin type B (Gel B)	60	4.8	C
Bovine serum albumin (BSA)	66.3	4.8	C
Streptavidin (Str)	53	5	C
Ovalbumin (Ova)	45	5.1	C
Human serum albumin (HSA)	69.4	5.2	C
Apolipoprotein E4 (Apo E4)	59	5.5	C
Lipase (Lip)	58	5.6	C
Hemoglobin (Hem)	64.5	6.8	C
Horseradish Peroxidase (HRP)	40	7.2	C
α-Chymotrypsin (ChT)	25	8.7	C
α-Chymotrypsinogen A (ChT A)	25.7	9	A
Gelatin type A (Gel A)	87.5	9.2	A
Ribonuclease A (Rib A)	13.7	9.4	A
Papain (Pap)	23	9.6	A
Cytochrome c (Cyt)	12	10.3	A
Avidin (Avi)	69	10.5	A
Trypsin (Trp)	23.3	10.5	A
Lysozyme (Lys)	14.4	11	A

Table S2. Hydrodynamic sizes of BSA-PCL-*b*-P2VP measured by DLS (a-c) with different mass ratios of proteins to PCL-*b*-P2VP ($M_{Protein}/M_{Polymer}$).

System	$M_{Protein}/M_{Polymer}$	Diameter (nm)
PCL-*b*-P2VP-BSA-1	0.57	186 ± 84
PCL-*b*-P2VP-BSA-2	0.29	221 ± 87
PCL-*b*-P2VP-BSA-3	0.11	260 ± 124

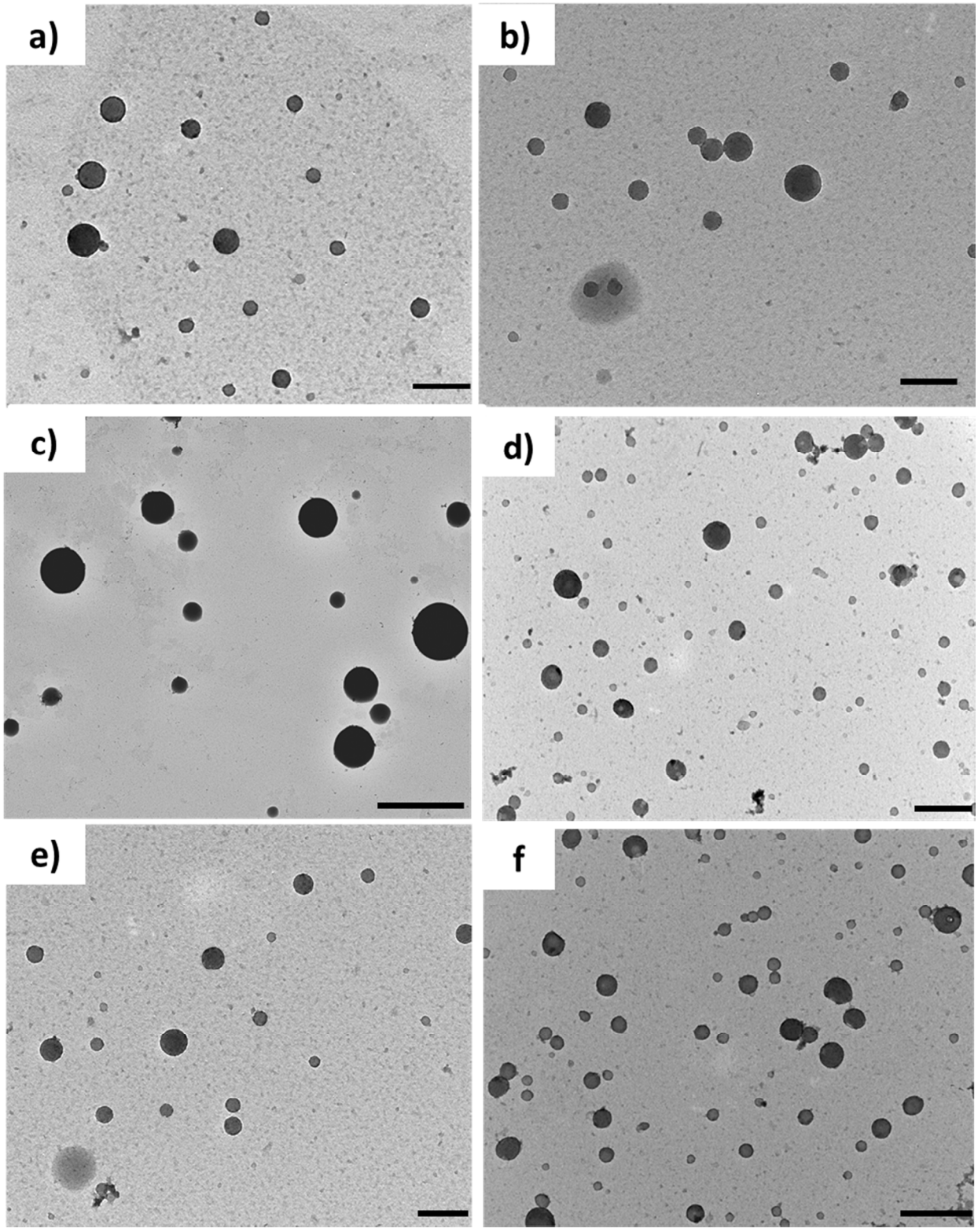

Figure S1. Representative TEM images of PPCS-NPs in PBS buffer. a) Lip-P4VP; b) HEM-P4VP; c) Myo-P4VP; d) Str-P4VP; e) Con A-P4VP; and f) Pep-P4VP. All scale bar = 500 nm.

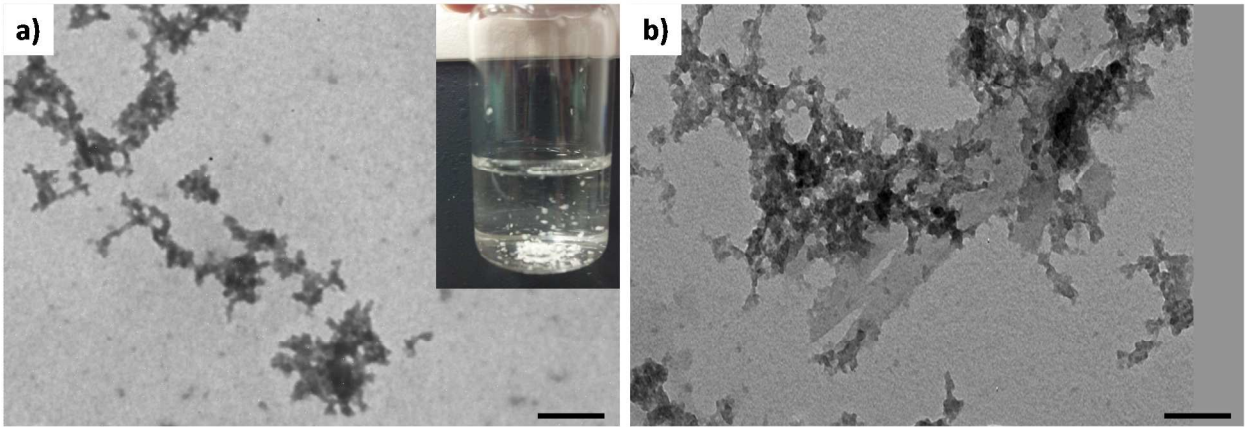

Figure S2. Representative TEM images. a) only P4VP in PBS buffer. The inset showed an optical image of the insoluble P4VP in PBS; b) Lys-P4VP in PBS buffer. The scale bar = 250 nm.

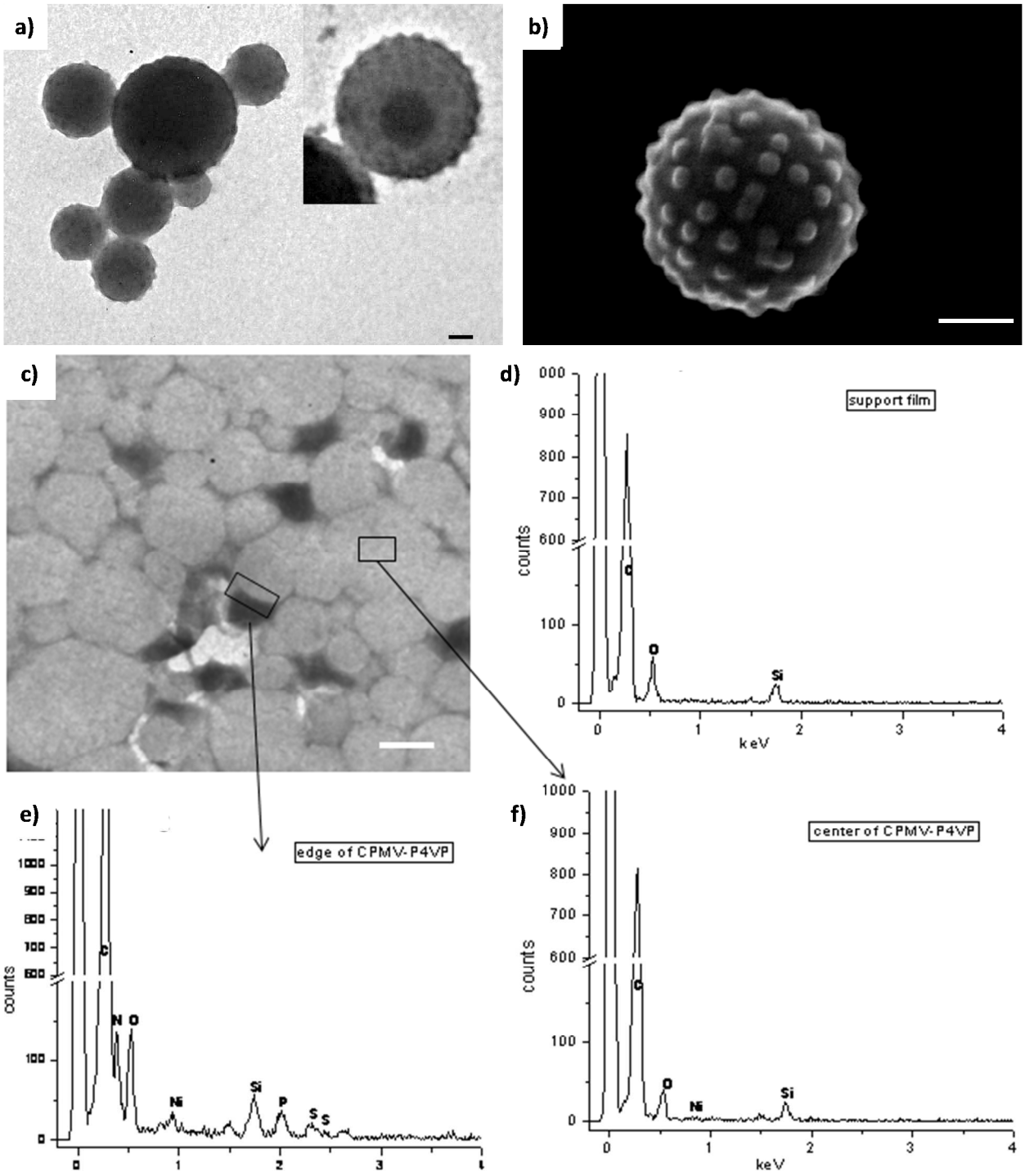

Figure S3. Structural analysis of PPCS-NPs using FESEM, thin-sectioned TEM and EDS. a-b) TEM and FESEM images of CPMV-P4VP. c) Unstained CPMV-P4VP thin section structures. d) EDS spectrum from the TEM supporting film, where Si was identified. e, f) EDS spectrum of the edge and the center area of the CPMV-P4VP, respectively. Scale bar = 100 nm.

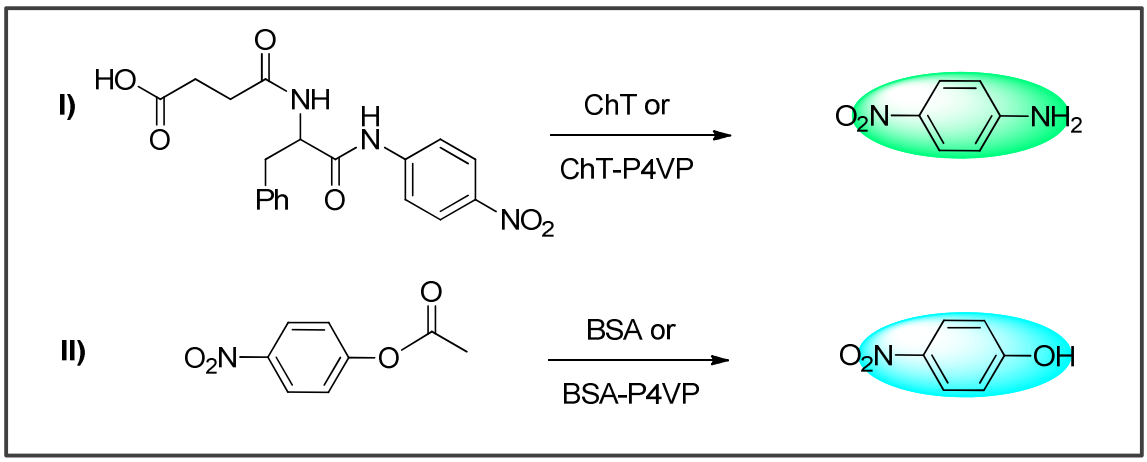

Scheme S1. **Schematic representative activity assay of I) ChT, II) BSA.** The fluorogenic products from the enzymatic hydrolysis of the substrates were monitored spectroscopically while the native enzymes were used as control studies.

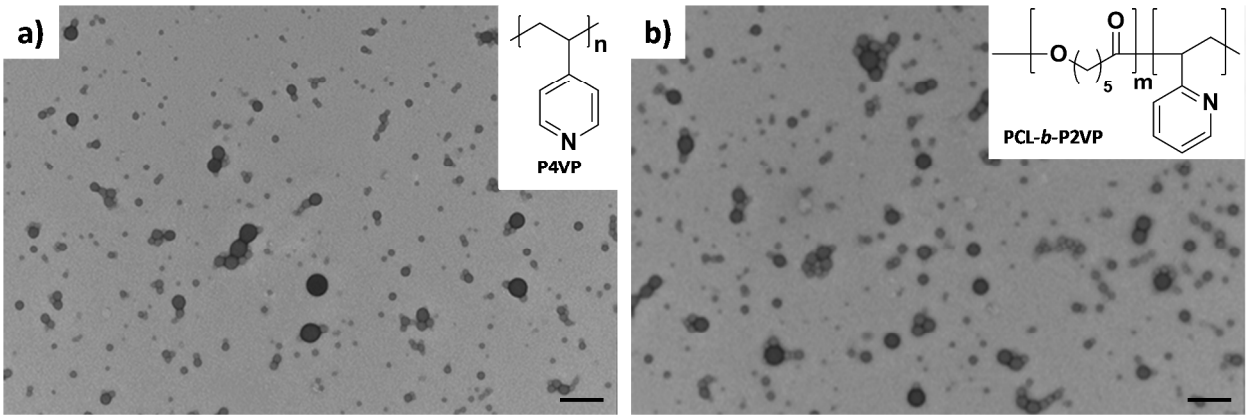

Figure S4. TEM representative of GOX-HRP assembled with a) P4VP and b) PCL-*b*-P2VP. The particles exhibit spherical structure with the size of about 150-250 nm in diameter. Scale bar = 500 nm.

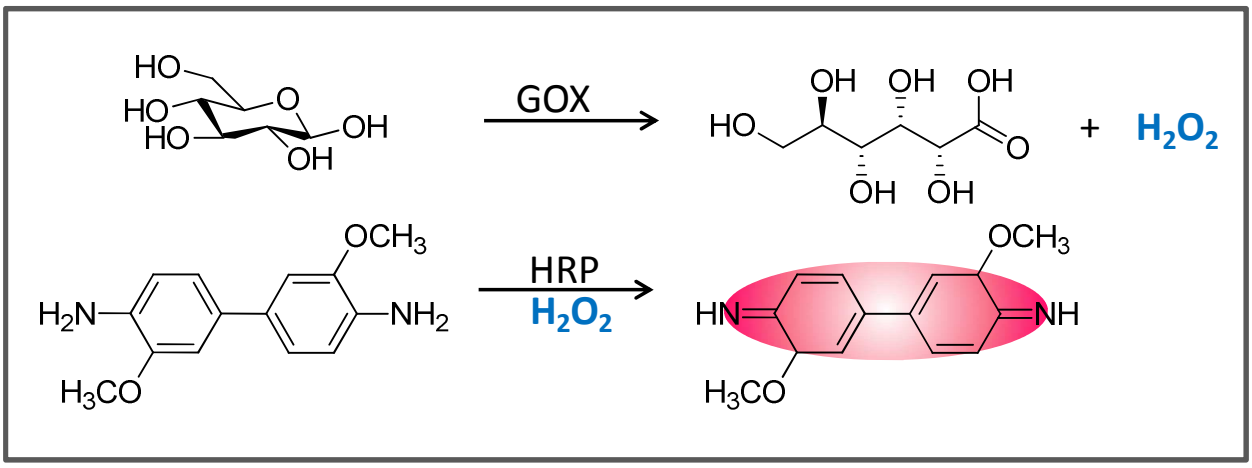

Scheme S2. **Schematic representation of the bienzyme cascade reaction of GOX and HRP.** In these sequential reactions, the peroxide, which is released from the oxidation of glucose with GOX, is sequentially reacted with HRP in the presence of o-dianisidine to yield an oxidized o-dianisidine.

Assembly of PPCS-NPs at different pH conditions

To investigate the effect of the pH on the protein structure after assembly, we checked the secondary structure of three different proteins after assemble at different pH. Under pH 2 where pH < pI of the BSA, no assembly was observed. The sample was then centrifuged to remove the white pellet which belongs to the polymer, then the supernatant was subjected to the analysis. As shown in Figure S5d, both native BSA and BSA-P4VP at pH 7 show two strong minima at 208 and 222 nm, which are corresponded to the α-helix of the BSA structure.[1] At pH 2, a decrease in intensity and a slight blue shift of these minima were observed. The structural changes of the BSA at pH 2 can be explained by acid denaturation of the protein. The ionizable protein groups (pKa > 3) are protonated under this condition, resulting in the unfolding of the protein molecules from charge repulsion.[2] At pH 10 where the assembly also occurs, a moderate disruption in the secondary structure which was a result of a loss of α-helix of BSA was observed. Although the change in secondary structure may not be clearly observed at such pH, severe loss in tertiary structure is often observed as previously report.[1]

The enzymatic activity of BSA in the hydrolysis of *p*-nitrophenyl acetate was also evaluated at different pHs. As shown in Figure S5c, the lowest activity was found at pH 2 where the BSA was suspected to be denatured. The activity was shown to increase as the pH of the solution increase, and the highest activity was found at pH 10 where both acetic and p-nitrophenol are fully ionized. However, such condition tends to lead to protein denaturation and protein unfolding in a long run.

CD analysis was also performed with two other proteins: Lip and ChT (Figure S5e, f). Lipase behaves similarly to BSA regarding its assembly behavior. Interestingly, Lip itself aggregates

within 2 hours at pH 10 whereas no aggregation was found after assembling with P4VP at this pH. We rationalize that due to a stronger interaction between protein and polymer, the polymer may help preventing proteins from agglomerating to each other, thereby prolonging the stability of the protein. For the CD spectroscopy, Lip-P4VP at pH 7 shows a strong minimum at ~203 nm, similar to that of the native Lip.[3] A slight loss of the minimum as well as a red shift was observed when exposing to pH 2 and 10, indicating a slight change in protein's secondary structure at these conditions. For a cationic protein, ChT was used, and the CD spectra show two strong minima at 202 and 230 nm.[4] However, upon exposing the ChT at pH 2 and 10, a significant decrease in both minima was observed, indicating the unfolding of the structure.

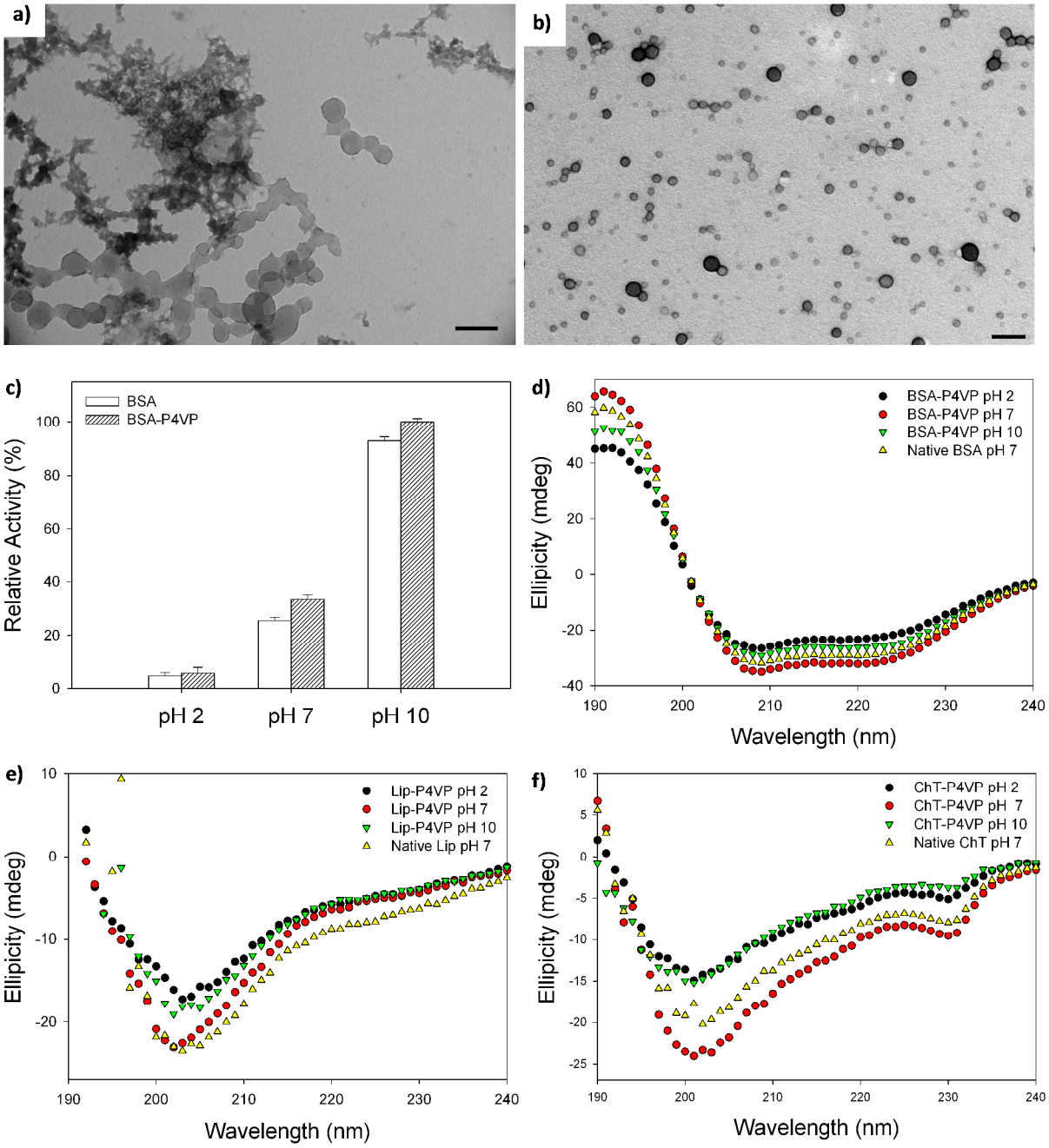

Figure S5. Representative TEM images, activity assay, and CD analysis of PPCS-NPs under different conditions. a) BSA-P4VP at pH 2; and b) BSA-P4VP at pH 10. All scale bar = 250 nm. c) Enzymatic activity of BSA and BSA-P4VP at pH 2, 7 and 10. d-f) Circular dichroism analysis of BSA-P4VP, Lip-P4VP, and ChT-P4VP at pH 2, 7, and 10, respectively, in comparison to the native proteins.

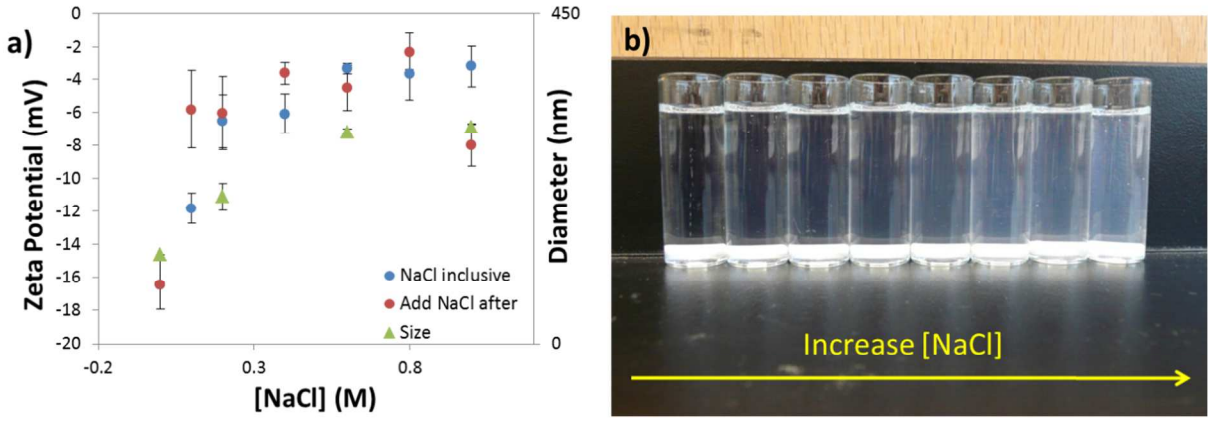

Figure S6. Mechanism investigation of the formation of PPCS-NPs. a) Ionic effect on the Zeta potential and size of the BSA-P4VP nanoparticles at pH 7.4. NaCl was added to BSA solution prior to assembly. b) Different concentration of NaCl (0-1.0 M) was incorporated prior to assembly. An increase in particle turbidity was observed as the ionic strength was increased, suggesting that the PPCS-NPs were stabilized by the electrosteric stabilization.

Synthesis of pyridine-derivatized pHEMA (10)

The synthesis was carried out via esterification of the hydroxyl group on pHEMA. Briefly, pHEMA (150 mg, 1.155 mmol OH residues) was dispersed in anhydrous THF (5 mL) at room temperature. DMAP (451 mg, 3.696 mmol) was added, and the mixture was allowed to stir at room temperature until the solution became homogeneous. To the solution mixture, nicotinoyl chloride hydrochloride (411 mg, 2.31 mmol) was added under N_2. The esterification was allowed to proceed at room temperature for 24 h. A precipitate appeared within 24 h and was separated from the liquid by centrifugation. The precipitate was further washed with THF, and the supernatant was combined together and precipitated in cold diethyl ether. The final solid was rinsed with cold methanol several times to remove excess DMAP. Finally, the precipitate was collected and dried in a vacuum oven at ambient temperature.

Synthesis of benzene-derivatized pHEMA (12)

pHEMA (300 mg, 2.31 mmol OH residues) was dispersed in anhydrous pyridine (5 mL) at room temperature. Benzoyl chloride (650 mg, 4.62 mmol) was added under N_2. The esterification was allowed to proceed at room temperature for 6 h, and white precipitation was evident. After that, the reaction mixture was heated to 80 °C under N_2 for 24 h, resulting in a homogeneous light yellow solution. The precipitation was evident after allowing the mixture to cool down at room temperature. The yellow supernatant was precipitated in cold diethyl ether resulting in white pellet, which was later dissolved in THF to give two liquid layers. The THF layer was extracted out and dried under vacuum. The final solid was rinsed with cold methanol several times to remove excess DMAP. Finally, the white solid was collected and dried in a vacuum oven at ambient temperature.

Synthesis of pyridine/benzene (1:1)-derivatized pHEMA (11)

pHEMA (150 mg, 1.155 mmol OH residues) and DMAP (12 mg, 0.098 mmol) were dispersed in anhydrous pyridine (20 mL) at room temperature. To the solution mixture, nicotinoyl chloride hydrochloride (214 mg, 1.2 mmol) and benzoyl chloride (168 mg, 1.2 mmol) were added under N_2. The esterification was allowed to proceed at room temperature for 6 h, and the reaction mixture was heated to 80 °C for 12 h to result in a light yellow liquid. The liquid was precipitated in cold diethyl ether to give white precipitation, which was further rinsed with cold methanol several times to remove excess DMAP. Finally, the precipitate was collected and dried in a vacuum oven at ambient temperature.

With the successful esterification of pHEMA with nicotinoyl chloride and benzoyl chloride, we then sought to exploit the property of this chemistry toward the self-assembly process. As aforementioned, we proposed that pyridine played a chief role in self-assembly. Therefore, **10** was synthesized to confirm our hypothesis while **12** was employed as an experimental control. In this section, the derivatiations of pHEMA with a variety of pyridine and benzene ratios were successfully prepared. The esterification of pHEMA with different ratios of nicotinoyl chloride/benzoyl chloride (NC/BC) were conducted as shown in **Figure S3a.** A detailed ratio of starting material was indicated in **Table S3**. It is noteworthy to point out that the sequence of the addition of acyl chloride is important in controlling the final ratio of the pyridine/benzene presented in the final product. When adding both nicotinoyl chloride and benzoyl chloride at the same time, the final product was more likely to have a 1:1 of pyridine/benzene. This was likely due to an equal chance of both residues to compete per one –OH unit on the pHEMA. In order to obtain a 4:1 ratio of pyridine/benzene in the final product, benzoyl chloride must be added to the reaction first. After allowing the reaction mixture to stir

overnight at room temperature, nicotinoyl chloride was added afterwards. The solvent used in each reaction is shown in **Table S3**. The products were purified by precipitation in cold diethyl ether and dried in vacuum prior to the analysis.

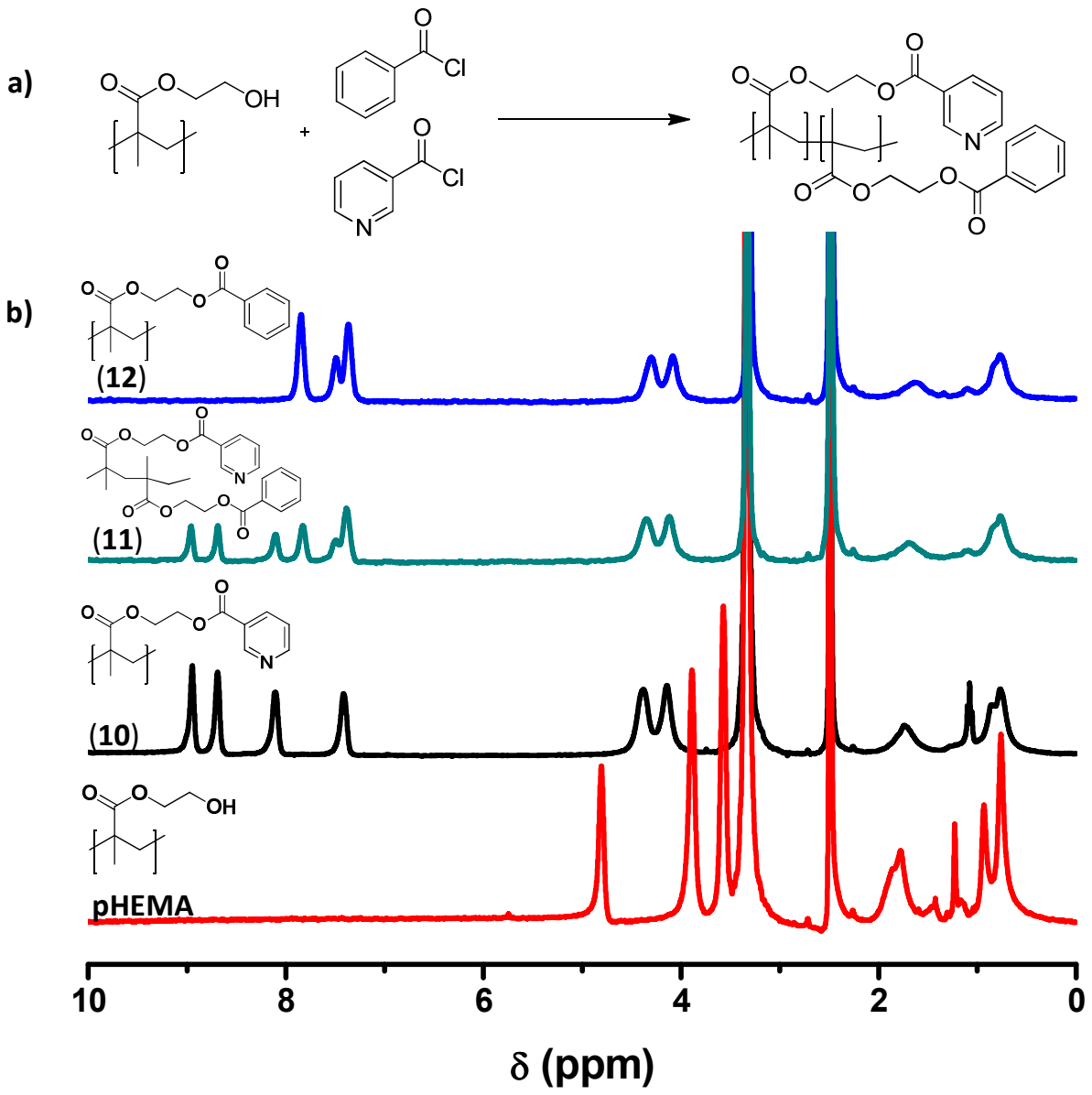

Figure S7. Esterification of pHEMA with different ratios of nicotioyl chloride/benzoyl chloride for the synthesis of polymer 10-12. The ratios of the final product were corresponded to **Table S3**. b) Representative ^{1}H-NMR spectra (DMSO-*d6*) of the derivatizations of pHEMA with different ratios of pyridine and benzene. The disappearance of –OH in both spectra suggests 100% derivatization.

Table S3. Esterification of pHEMA with different ratios of nicotinoyl chloride/benzoyl chloride. This table is corresponded to ***Figure 3***NC/BC = nicotinoyl chloride/benzoyl chloride

Polymer	NC/BC molar ratio	% yield	H_2O[a]	Methanol	DMSO	DMF	THF
pHEMA	-	-	+	+	+	+	-
(10)	1:0	> 90	-	-	+	+	+
(11)	1:1	> 90	-	-	+	+	+
(12)	0:1	> 90	-	-	+	+	+

[a] + = soluble, - = insoluble

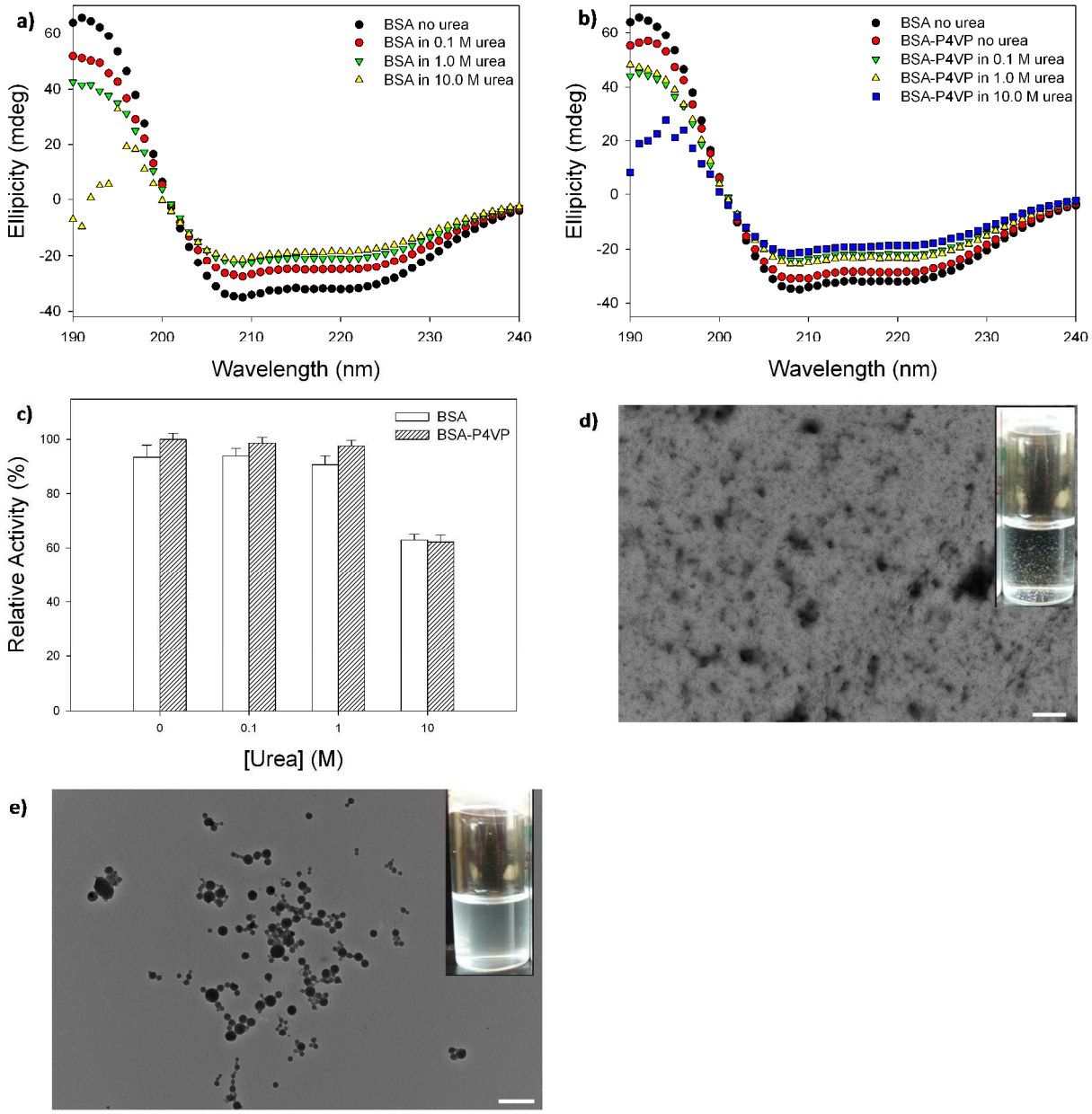

Figure S8. CD spectra and relative activity of BSA exposed to different urea concentration. a, b) CD spectra of BSA and BSA-P4VP in 0, 0.1, 1, and 10 M urea. c) Relative activity of BSA and BSA-P4VP in 0, 0.1, 1, and 10 M urea. d, e) TEM images of the assembly of BSA and P4VP with the presence of urea (0.1 M) , and when the BSA was heated at 95 °C for 10 min, respectively. Scale bar = 500 nm.

References

(1) Estey, T.; Kang, J.; Schwendeman, S. P.; Carpenter, J. F. *J. Pharm. Sci. 2006, 95*, 1626.
(2) Goto, Y.; Takahashi, N.; Fink, A. L. *Biochemistry* **1990**, *29*, 3480.
(3) Karkhane, A. A.; Yakhchali, B.; Jazii, F. R.; Bambai, B. *J. Mol. Catal. B: Enzym.* **2009**, *61*, 162.
(4) De, M.; Rotello, V. M. *Chem. Commun.* **2008**, 3504